PROCEEDINGS, Thirteenth Workshop on Geothermal Reservoir Engineering
Stanford University, Stanford, California, January 19-21, 1988
SGP-TR-113

TRANSIENT BEHAVIOR IN FRACTURED MEDIA WITH ZERO MATRIX PERMEABILITY

E.Okandan, J.Öngen, M.Arpacı

Petroleum Engineering Dept.,METU, TURKEY

ABSTRACT

Pressure transient analysis is one of the powerful tools that provides estimates on in-situ reservoir properties. Development of theory since 1935 from the classic paper of Theis, has provided analysis procedures for different pressure tests in wells. The solutions to respective partial differential equations for dual porosity or fractured systems also found wide application in estimating reservoir properties in geothermal reservoirs.

When we analyze the response of a reservoir to pressure disturbances, we assume a model to simulate the system, and properties are estimated from the best fit to this model. The present paper will discuss some experimental results obtained from a fractured medium with zero matrix permeability, where dimensions of blocks, fracture spacing, exact location of production points and reservoir size are known. The pressure transient data obtained from a laboratory geothermal model, were analyzed using conventional analysis techniques. The results imply, even for this fully fractured system, the reservoir behaves as if it has the properties of a dual porosity medium. Several tests conducted at different rates and at different production depths resulted in similar kh and $\phi C_t h$ values, indicating that the parameters affecting the pressure transients were the overall properties of the medium.

In this paper only drawdown tests will be presented.

INTRODUCTION

Geothermal reservoirs are generally fractured rocks and their matrix permeabilities may be negligibly small. In such cases the flow will be mainly through fractures and transient behavior will depend on the fracture network and fracture properties.

Laboratory experiments were designed to obtain pressure transient data for a specific fracture geometry where marble matrix blocks had no permeability. The orientation of blocks was such that there was flow connection between all fractures and the injection-production points. Two different block sizes were chosen (Fig.1.a, Fig 1.b). The details of the experimental set up were given elsewhere (1,2).

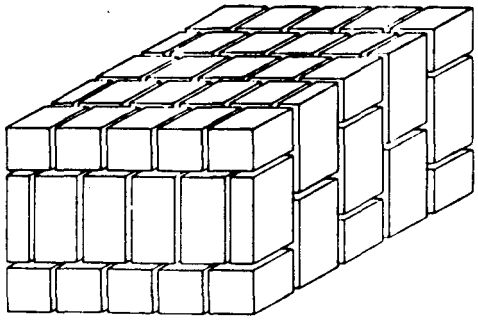

Model A

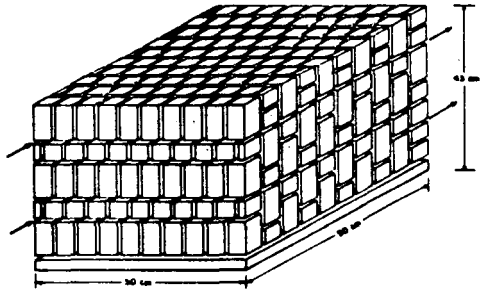

Model B

Fig. 1. Packing of marble blocks in the experimental set up.

EXPERIMENTAL CONDITIONS

The reservoir model was heated upto 110 C and to a pressure above boiling pressure, then the selected ports for injection and production were connected to measuring equipment. An initial drawdown test was followed by an interference test where pressure rise at the producing end was recorded while cold water was injected at constant rate. This was followed by another drawdown test. The location of injection and production ports were changed in order to create different flow paths and observe their effect on transient behavior. The flow rates ranged between 20 cc/min to 60 cc/min on both models. The fracture spacing created by the big blocks were 10 cm and it was 5 cm in the pack created by smaller blocks.

RESULTS AND DISCUSSION

In both models due to the packing of marble blocks flow paths are connected and continuous and it was expected to see the effect of fractures intersecting the production ports. The transient behavior should reflect the fracture density as well as the limited volume of the models.

In both models, the shapes of both semi-log and log-log plots characterized a dual porosity system (Fig.2, Fig.3). The late time data were checked if increase in ΔP was due to pseudo steady state flow. For all experiments, the data did not follow a unit slope straight line on log ΔP versus log t plot, where the second semi-log straight line was observed. So the flow behavior is due to the dual porosity effect created in the models.

In the analysis of the data, the $(kh)_f$ value estimated from the semi-log straight line was used to find the pressure match for the log-log type curve. The best fit to $(C_D\, e^{2S})_f$; λe^{2S} and $(C_D\, e^{2S})_{f+m}$ were obtained for each drawdown data obtained from different production ports (3).

Since production was obtained from a point without a wellbore the effect of wellbore storage and skin was absent.

Therefore the match obtained on $(C_D\, e^{2S})$ curves are basically equal to C_D. The flow period which corresponds to first $(C_D)_f$ curve is due to the main preferential fracture path leading to the production point, this main path is fed from auxiliary fractures whose overall affect is reflected in the second C_D curve. The values of λ and w then indicate the relationships between the medium made up of these auxiliary flow paths and main flow path.

From the type curve match, average $(C_D)_f$ values for model A, larger blocks, were 4 while for model B it was 1. Similarly $(C_D)_{f+m}$ for model A was 0.75 and for model B, 0.45 (Table 1). This indicated that the storativity was higher in the large block model. This concluison was also reflected in the w values that were calculated. For model B w was higher than model A.

The storage was determined from the time match. Since there was no wellbore, the storage observed is due to the fissures intersecting the production port.

The fractures created by larger blocks (Model A) exhibited larger storage average being 3.25×10^{-9} m^3/Pa compared to 2.23×10^{-9} m^3/Pa in smaller blocks. Permeability was also high in Model A. In Table 1, only $(k,h)_f$ values are reported since h which is the effective height open to flow was not very easy to define for the models under consideration.

$(\phi c_t\, h)_f$, as determined from the $(C_D)_f$ match and from semi-log analysis had shown some differences. This is due to uncertainly in matching the initial data to the first $(C_D\, e^{2S})$ curve. However order of magnitude values for both models were similar.

The λ values determined from the type curve, assuming skin to be zero was slightly higher for model B. Since geometric shape of blocks and fractures were similar, the slight difference is due to $(kh)_m/(kh)_f$ values which correspond to auxilary flow path conductance to main flow path conductance in the present models.

Drawdown tests conducted before and after an interference test showed very similar behavior exhibiting the reproducibility of data (4,5).

Experimental data obtained at different production depths, expressed as H_p measured from bottom as a fraction of total depth, was not different , (Fig. 4,5) because the geometry of the fractures were the same and their distribution was similar. However, tracer experiments conducted on both models, showed varying dispersions as the injection and production depths were changed (2,5).

Concentration profiles of tracer returns also indicate a main fracture flow path and later auxiliary fractures feeding to it. As the fracture density was increased (model B) the dispersion was higher. (Fig.6,7) and it was reflected in the tracer profiles obtained at different production points.

CONCLUSION

Model experiments on two fractured reservoir models with zero matrix permeability, showed the transient behavior was similar to a double porosity system.

Increased fracture density in small

block model, caused $(kh)_f$ values to be smaller which also affected λ, interporosity flow parameter to become slightly higher as compared to larger blocks.

Storativity of the main fracture flow system was high in the model that had more fractures and smaller block sizes.

Geothermal reservoirs which generally produce fluid through fractures may exhibit dual porosity behavior even the matrix may have very low or effectively zero permeabilities. The minor or auxiliary fractures that contribute to the flow in the main fracture system, will act as the less permeable medium of a dual porosity model.

NOMENCLATURE

$$C_D e^{25} = \frac{0.8936.\ C\ e^{25}}{\phi C_t\ h\ r_w^2}$$

$$\lambda e^{-25} = \alpha r_w^2 .\ \frac{k_m}{k_f}\ e^{-25}$$

$$W = \frac{(C_D\ e^{25})_{f+m}}{(C_D\ e^{25})_f} = \frac{(\phi C_t\ h)_f}{(\phi C_t\ h)_{f+m}}$$

REFERENCES

1. Hosca, H., Okandan, E. (1986), "Reinjection Model Studies in Fractured and Homogeneous Geothermal Systems", Proceedings Eleventh Workshop Geothermal Reservoir Engineering, Jan. 21-23, 1986.
2. Bayar, M., Okandan, E.(1987), "Tracer Flow In a Fractured Geothermal Reservoir Model" Proceedings Twelfth Workshop on Geothermal Reservoir Engineering, Jan. 20-22, 1987.
3. Bourdet, D., Gringarten, A.C. (1982), "Determination of Fissure Volume and Block Size in Fractured Reservoirs by Type-curve Analysis", SPE paper no. 9293, 1982.
4. Öngen, J. (1987), "Interpretation of pressure Data in a Three Dimensional Fractured Reservoir Model", MSc.Thesis 1987, Petroleum Eng.Dept., METU
5. Arpacı, M. (1988), "Transient and Tracer Behavior in Fractured Geothermal Model with Zero Matrix Permeability", MSc.Thesis 1988, Petroleum Eng.Dept., METU

TABLE 1. Semi-log and Log-log Analysis of Some Pressure Transient Data Obtained on Model A and B.

			Semi-log Analysis		Log-log Analysis				
H_p		Test No	kh, md-ft	$(\phi C_t\ h)_f$ m/Pa	λ	w	$(\phi C_t\ h)_f$	$(C_D)_f$	$(C_D)_{f+m}$
0.25	Model A								
		41	4.46	81×10^{-6}	0.1	0.25	55×10^{-6}	2	0.5
		30	5.74	78.7×10^{-6}	0.15	0.3	30×10^{-6}	3	1
	Model B								
		FDW-1	2.75	59.3×10^{-6}	0.14	0.5	56.5×10^{-6}	1	0.5
		FDW-4	2.49	78.7×10^{-6}	0.12	0.34	66.5×10^{-6}	1.5	0.5
		IDW-1	2.45	60.2×10^{-6}	0.14	0.5	44.1×10^{-6}	1.5	0.4
0.75	Model A								
		27	3.24	105×10^{-6}	0.15	0.14	50.8×10^{-6}	5	0.7
		36	2.29	43.7×10^{-6}	0.1	0.1	17.3×10^{-6}	5	0.5
	Model B								
		FDW-2	2.42	64.9×10^{-6}	0.20	0.3	69.3×10^{-6}	1	0.3
		FDW-3	2.16	64.1×10^{-6}	0.16	0.5	68.2×10^{-6}	1	0.5

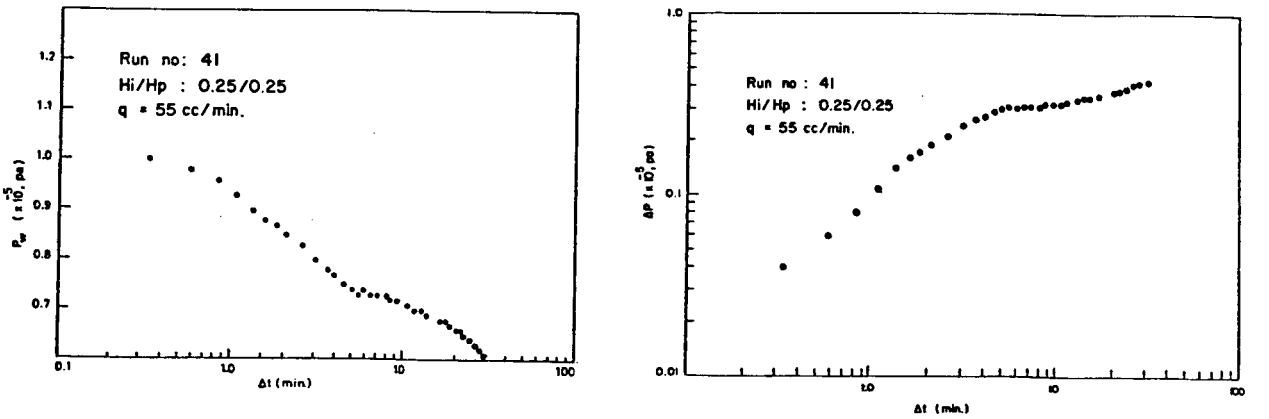

Figure 2. Pressure Drawndown Obtained on Model A at H_p of 0.25 (Test#41)

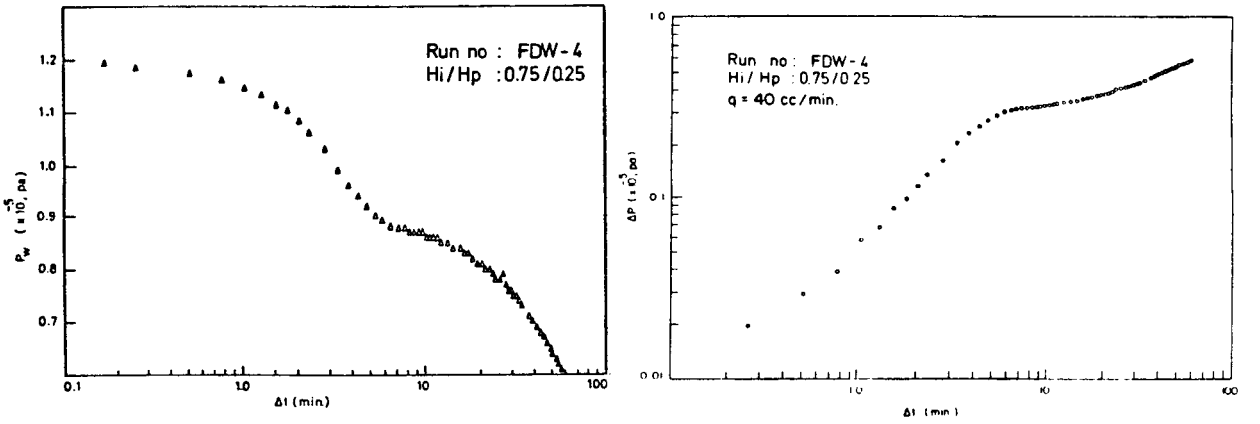

Figure 3. Pressure Drawndown Obtained on Model B at H_p of 0.25 (Test FDW-4)

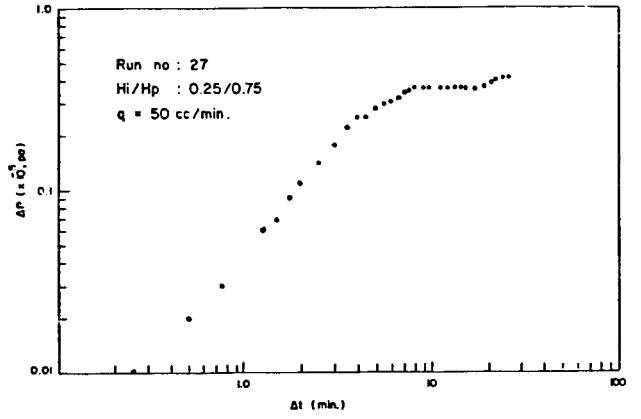

Figure 4. Transient Behavior at H_p of 0,75 for Model A (Test #27)

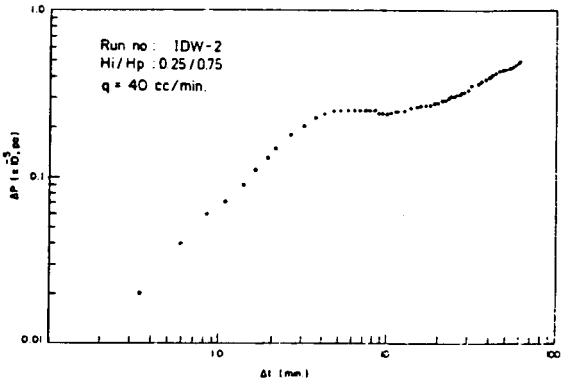

Figure 5. Transient Behavior at H_p of 0.75 for Model B (IDW-2)

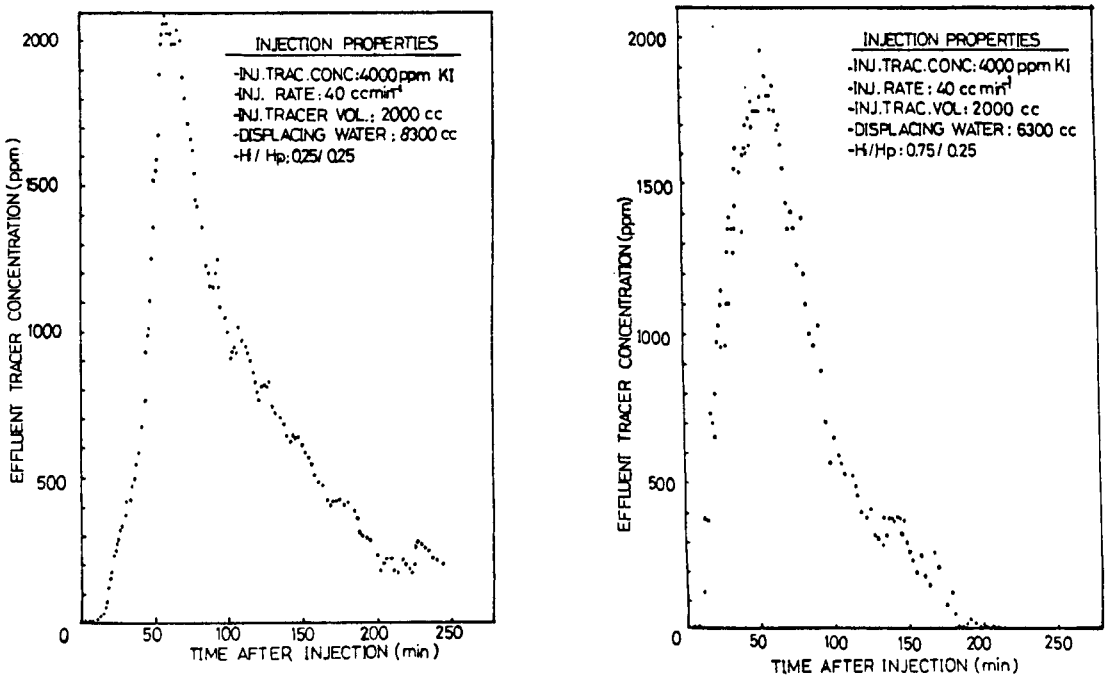

Figure 6. Tracer Production Profile in Model A for H_i/H_p of 0.25/0.25 and 0.75/0.25

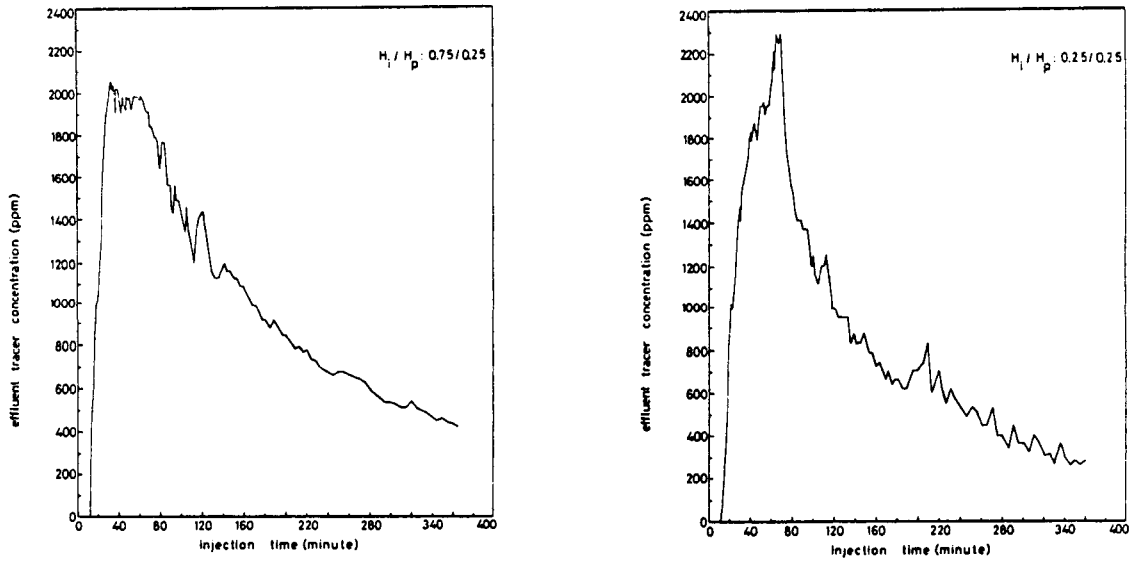

Figure 7. Tracer Production Profile in Model B for H_i/H_p of 0.25/0.25 and 0.75/0.25